THE IMPACT OF BUILDINGS' CHARACTERISTICS ON AIRFLOW PATTERNS AND BED MORPHOLOGY AT BEACHES, USING CFD MODELLING

Paran Pourteimouri, University of Twente, p.pourteimouri@utwente.nl
Geert Campmans, University of Twente, g.h.p.campmans@utwente.nl
Kathelijne Wijnberg, University of Twente, k.m.wijnberg@utwente.nl
Suzanne Hulscher, University of Twente, s.j.m.h.hulscher@utwente.nl

INTRODUCTION

During the last century rapid urbanization of coastal zones has been widespread all over the world. This highly increasing population in coastal zones leads to the construction of restaurants, sailing clubs, beach houses and pavilions at the beach-dune interface. Structures located adjacent to dunefields change the local airflow patterns which, in turn, alter sediment transport pathways and influence the aeolian landforms [Jackson and Nordstrom, 2011]. Figure 1 schematically shows the mean flow field around an isolated cubical building with an orientation perpendicular to the incident wind flow. As shown in Figure 1, the flow field contains complex recirculation zones in front of the building, over the roof of the building, around the lateral sides of the building and in the downstream cavity region just behind the rear face of the building.

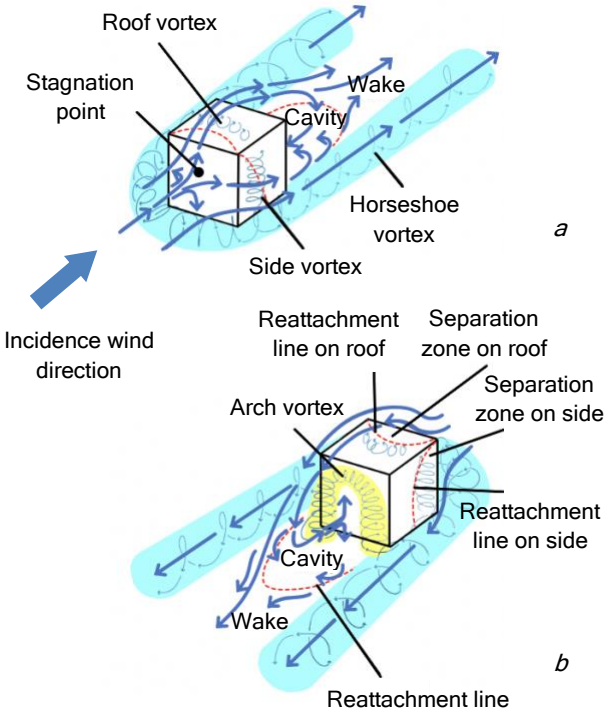

Figure 1 - Airflow patterns around an isolated cubical building *a*) windward view, and *b*) leeward view (modified from Blocken et al., 2011 and Oke et al., 2017).

The significant effects that the buildings' characteristics at beaches can have on local airflow patterns, and consequently on sediment transport and bed morphology are still not fully understood. In this paper, firstly the impacts of buildings' characteristics on airflow patterns are investigated, specifically the impacts of building length, width and height. Secondly, the near-bed horizontal divergence of the velocity field is calculated for one case to infer resulting erosion and deposition patterns around the building. For all these purposes, a numerical model is developed.

METHODOLOGY

A three-dimensional computational fluid dynamics (CFD) model making use of OpenFOAM, an open-source CFD solver, is developed to solve the wind flow around an isolated cubical building. Considering the wind flow as incompressible in this study, the simpleFoam solver in OpenFOAM is used. The simpleFoam algorithm is recommended for steady-state simulation of turbulent flows and it solves the Navier-Stokes equations using the finite-volume method (FVM) and an approximated solution for solving the turbulence, namely Reynolds-averaged Navier-Stokes (RANS) approach. The governing equations of the incompressible flow field can be expressed by continuity and momentum equations that can be written in their steady-states as the following equations, respectively:

$$\nabla.\vec{U} = 0 \qquad [1]$$

$$(\vec{U}.\nabla)\vec{U} = -\nabla p_k + \nabla.(\upsilon_{eff}\nabla\vec{U}) \qquad [2]$$

where $\vec{U}\ [m/s]$ is the flow velocity vector; $p_k\ [\mathrm{m}^2/s^2]$ is the kinematic pressure, defined as the ratio of the static pressure, p_s, to the flow density, ρ; $\upsilon_{eff}\ [m^2/s]$ is the effective kinematic viscosity, defined as the sum of the kinematic viscosity of the flow, υ, and the kinematic turbulent viscosity, υ_t, which is calculated from the turbulence model. In this study, the well-known standard k-ε model proposed by Launder and Spalding (1974) is used, assuming that the impacts of turbulence on flow can be expressed by an increased viscosity, υ_t. This turbulent viscosity can be calculated by the turbulence kinetic energy, k, and its rate of dissipation, ε, as proposed by Richards and Hoxey, 1993:

$$\upsilon_t = C_\mu \frac{k^2}{\varepsilon} \qquad [3]$$

where C_μ is a dimensionless constant equal to 0.09. In the above equation, the values of k and ε are computed from their transport equations.

COMPUTATIONAL DOMAIN

A three-dimensional computational domain, shown in Figure 2, with the length of $5\ m$, width of $0.65\ m$ and height of $0.1\ m$ is considered for modelling airflow patterns around an isolated rectangular building. The building length, width and height are $0.1\ m \times 0.15\ m \times 0.125\ m$, respectively. The computational domain is symmetric in the spanwise directions. The inlet of the domain is located $1\ m$ upstream of the building centerline, while the domain outlet is located $4\ m$ downstream of the building centerline. The values are selected based on the wind-tunnel experiments done by Leitl and Schatzmann (2010) that their measurements are used for the model validation.

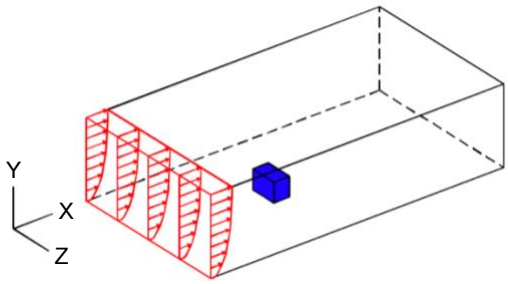

Figure 2 - Numerical computational domain including a rectangular surface-mounted building.

BOUNDARY CONDITIONS

The fully-developed profiles of mean wind speed, U, turbulence kinetic energy, k, and turbulence dissipation rate, ε, are introduced at the domain inlet using the following equations by Richards and Hoxey (1993):

$$U(y) = \frac{u^*}{\kappa} ln\left(\frac{y - y_g + y_0}{y_0}\right) \quad [4]$$

$$k(y) = \frac{u^{*2}}{\sqrt{C_\mu}} \quad [5]$$

$$\varepsilon(y) = \frac{u^{*3}}{\kappa(y - y_g + y_0)} \quad [6]$$

where $u^*\ [m/s]$ is the friction velocity, κ is the von Karman constant defined as 0.41 in OpenFOAM, $y\ [m]$ is the vertical coordinate, $y_g\ [m]$ is the ground level, $y_0\ [m]$ is the aerodynamic roughness length, and C_μ is the dimensionless constant in the standard $k - \varepsilon$ model. The following equation proposed by Richards and Hoxey (1993) is used to calculate the friction velocity in the above equations:

$$u^* = \frac{\kappa\, u_{ref}}{ln\left(\frac{z_{ref} + z_0}{z_0}\right)} \quad [7]$$

where u_{ref} is the reference velocity at a reference height, z_{ref}. The logarithmic boundary layer parameters used in this study, are defined in Table 1.

Table 1 - Values of the atmospheric boundary layer parameters.

$y_g\ [m]$	$y_0\ [m]$	$u_{ref}\ [m/s]$	$z_{ref}\ [m]$
0.0	0.0007	6.0	0.5

MODEL VALIDATION

For the model validation, the numerical results of the vertical velocity profiles in the vicinity of a building are compared with the wind-tunnel measurements performed by Leitl and Schatzmann (2010). The comparisons in Figure 3 are given at the symmetry plane ($z = 0.325\ m$):

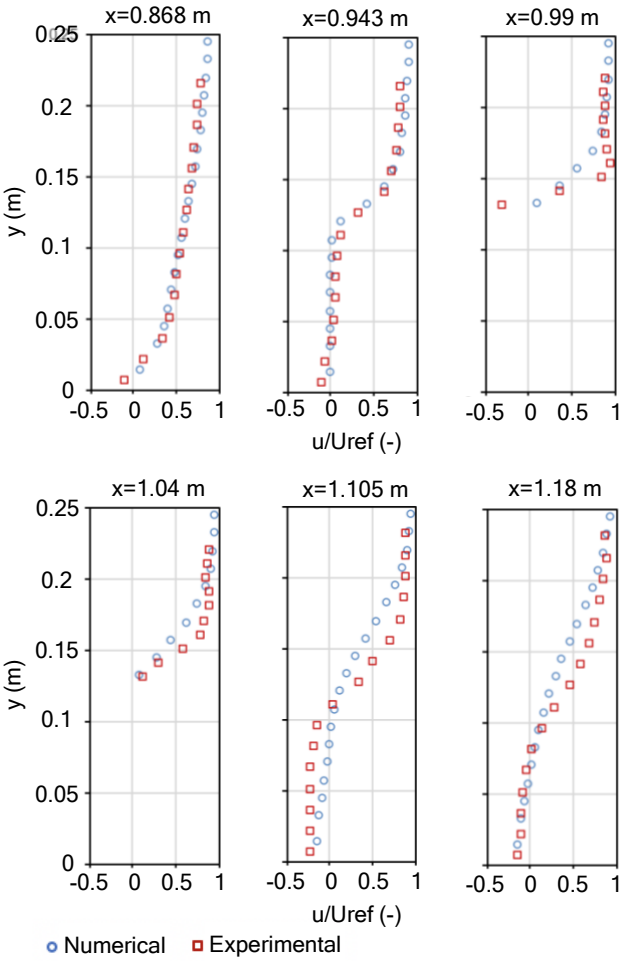

Figure 3 - Comparisons between numerical predictions of the vertical wind velocity profiles and wind-tunnel measurements at the symmetry plane ($z = 0.325\ m$).

RESULTS AND DISCUSSION

The impacts of building length, width and height are investigated in figures 4, 5 and 6, respectively. For this purpose, the reference building with the length of $0.1\ m$, width of $0.15\ m$ and height of $0.125\ m$ is used. The reference building is then increased in length, width and height up to three times the reference quantity in order to systematically investigate their influence. The results of

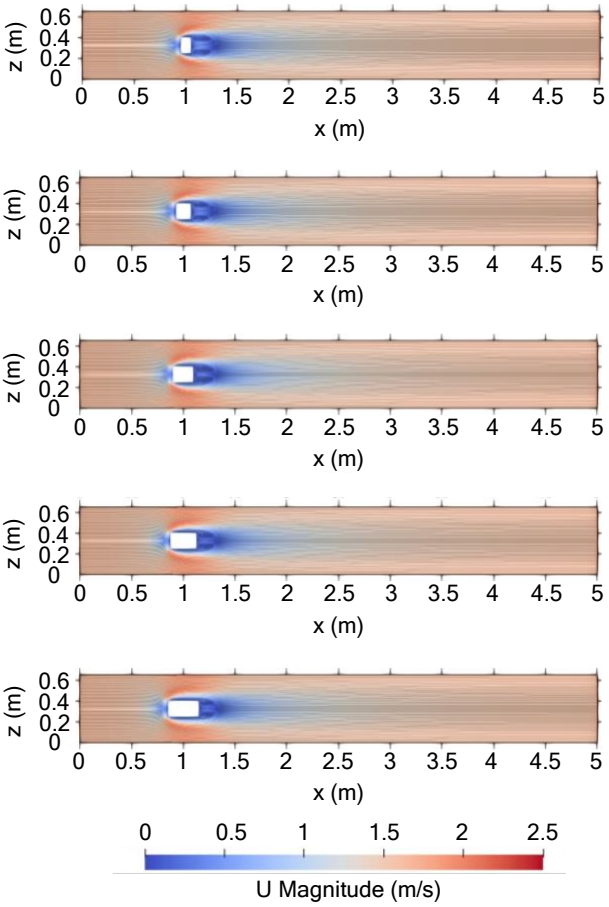

Figure 4 – The impacts of building length on airflow patterns at the horizontal plane at an elevation of y=0.0125 m.

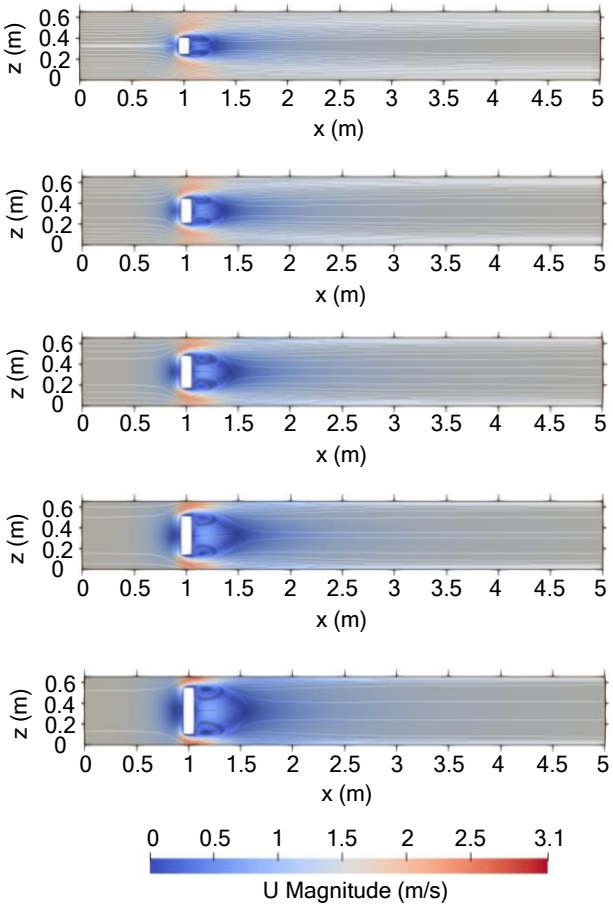

Figure 5 – The impacts of building width on airflow patterns at the horizontal plane at an elevation of y=0.0125 m.

airflow patterns and wind velocity magnitudes around the buildings are given at the horizontal plane at an elevation of $y = 0.0125\ m$ from the ground level. The results show that the airflow patterns around the building are least dependent on the length of the building in the wind direction. It can be concluded by comparing the models in Figure 4 with respect to the length of the upwind circulation zone in front of the building, downwind circulation zone (cavity region) behind the building and the overall length downstream the building that is influenced by the presence of the building. Furthermore, the results show that the airflow patterns around the building depend most on the width of the building normal to the wind direction. According to Figure 5, a wider building creates a longer and wider upwind circulation zone in front of the building and a longer and wider downwind circulation zone behind the building. In addition, a wider building impacts a longer distance downstream the building. Therefore, the velocity deficits continue for a longer distance behind the building when the building width increases.

The results show that the height of the building is also important for the airflow patterns around the building. According to Figure 6, the length of the upwind circulation zone in front of the building and the downwind circulation zone behind the building increases with increasing the height of the building. Furthermore, a higher building impacts the wind velocity magnitudes for a longer distance downstream the building.

The horizontal divergence of the velocity field is then calculated for one case, shown in Figure 7a, and the results are compared with the field measurements of erosion and sedimentation patterns around scaled buildings at the beach, shown in Figure 7b, done by Poppema et al. (2019). The divergence of the velocity field represents the rate of flow inward or outward from a given point, therefore the results of the horizontal divergence of the velocity field can be helpful for predicting the aeolian erosion and deposition patterns around a building. When the horizontal divergence in a given point is positive, it can be concluded that the rate of change of flow is outward and it is expected to see erosion in that point. The negative horizontal divergence in a given point shows that the rate of change of flow is inward and the sedimentation is more probable to happen in that point. Figure 7a shows that,

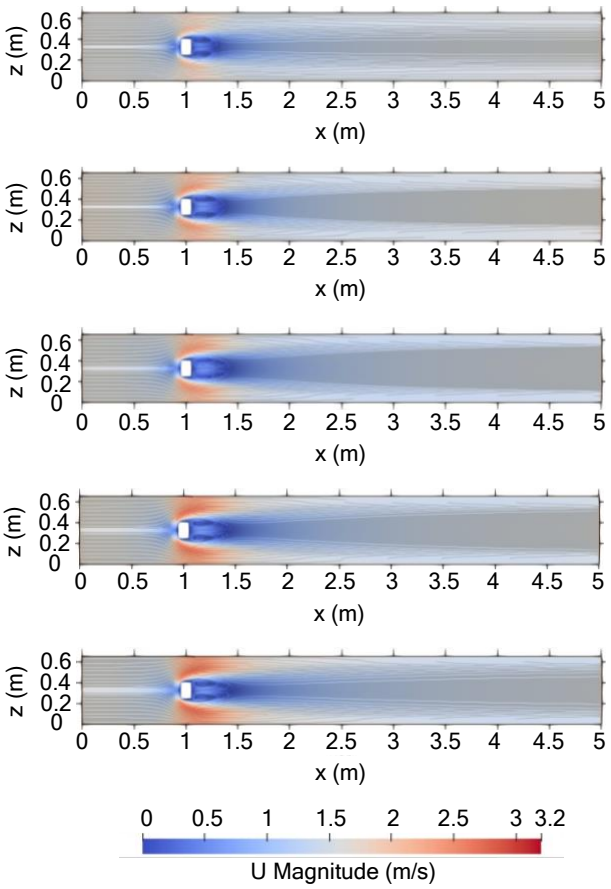

Figure 6 - The impacts of building height on airflow patterns at the horizontal plane at an elevation of y=0.0125 m.

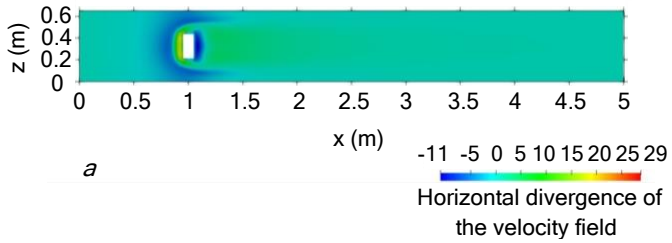

Figure 7 - Results of the *a*) numerical predictions of the horizontal divergence of the velocity field, and *b*) field measurements of erosion and deposition patterns around a scaled building (Poppema et al., 2019).

upwind the building and close to the building front face, the values of the horizontal divergence of the velocity field are positive, therefore it is expected that the erosion happens in those areas. In addition, the highest values of the horizontal divergence of the velocity filed occurs around the upwind edges of the building, meaning that it is expected to see an extensive erosion around the upwind edges of the building. There is a horseshoe-shape area in front of the building with negative values of the horizontal divergence of the velocity field, where it is expected to see sedimentation in those area. The deposition is also expected for a small area just behind the rear face of the building, where the negative values of the horizontal divergence of the velocity field happens. Downwind the building and between the two tails of the horseshoe-shape area in Figure 7a, the positive values of the horizontal divergence of the velocity field increases the possibilities for occurring erosion in those areas. Qualitative comparison between the numerical results of the horizontal divergence of the velocity field shown in Figure 7a, and the field measurements of the erosion and deposition patterns shown in Figure 7b, shows that the results are comparable.

ACKNOWLEDGEMENT
This work is part of the research programme ShoreScape, which is financed by the Dutch Research Council (NWO) and co-funded by RWS and HHNK.

REFERENCES

Blocken, B., Stathopoulos, T., Carmeliet, J., & Hensen, J. L. (2011). Application of computational fluid dynamics in building performance simulation for the outdoor environment: an overview. Journal of Building Performance Simulation, 4(2), 157-184.

Jackson, N. L., & Nordstrom, K. F. (2011). Aeolian sediment transport and landforms in managed coastal systems: a review. Aeolian research, 3(2), 181-196.

Launder, B. E., & Spalding, D. B. (1974). The Numerical Computation of Turbulent Flows. Computer Methods in Applied Mechanical Engineering, 3, 269-289.

Leitl, B., & Schatzmann, M. (2010). Cedval at hamburg university. URL http://www. mi. uni-hamburg. de/cedval.

Oke, T. R., Mills, G., Christen, A., & Voogt, J. A. (2017). Urban climates. Cambridge University Press.

Poppema, D. W., Wijnberg, K. M., Mulder, J. P. M., & Hulscher, S. J. M. H. (2019). Scale experiments on aeolian deposition and erosion patterns created by buildings on the beach Coastal Sediments 2019 (pp. 1693-1707): WORLD SCIENTIFIC.

Richards, P. J., & Hoxey, R. P. (1993). Appropriate boundary conditions for computational wind engineering models using the k-ε turbulence model. In Computational Wind Engineering 1 (pp. 145-153). Elsevier.